

8-25-2002

# Dielectric properties of a ferroelectric copolymer Langmuir–Blodgett film


Mahantappa S. Jogad

*Sharanabasaveshwar College of Science, Gulbarga, India, mahjogad@rediffmail.com*

Stephen Ducharme

*University of Nebraska, sducharme1@unl.edu*

Follow this and additional works at: <http://digitalcommons.unl.edu/physicsducharme>

 Part of the [Condensed Matter Physics Commons](#), and the [Polymer and Organic Materials Commons](#)

---

Jogad, Mahantappa S. and Ducharme, Stephen, "Dielectric properties of a ferroelectric copolymer Langmuir–Blodgett film" (2002).  
*Stephen Ducharme Publications*. 59.  
<http://digitalcommons.unl.edu/physicsducharme/59>

This Article is brought to you for free and open access by the Research Papers in Physics and Astronomy at DigitalCommons@University of Nebraska - Lincoln. It has been accepted for inclusion in Stephen Ducharme Publications by an authorized administrator of DigitalCommons@University of Nebraska - Lincoln.

## Dielectric properties of a ferroelectric copolymer Langmuir–Blodgett film

Mahantappa S. Jogad<sup>\*†</sup> and Stephen Ducharme<sup>#</sup>

<sup>\*</sup>Sharanabasaveshwar College of Science, Gulbarga 585 103, India

<sup>#</sup>Department of Physics and Astronomy, University of Nebraska, Lincoln, NE 68588-01111, USA

**We report measurements of the real ( $\epsilon'$ ) and imaginary ( $\epsilon''$ ) parts of the relative complex permittivity of a Langmuir–Blodgett film of ferroelectric copolymer of vinylidene fluoride (70%) with trifluoroethylene (30%). The measurements were made in the temperature range of 35 to 125°C, and frequency range of 19 Hz to 5 MHz. The results indicate low frequency loss due to conduction and dielectric loss peak near the ferroelectric–paraelectric phase transition.**

CRYSTALLINE ferroelectric polymers were discovered over thirty years ago, and typical samples made by solvent casting and spin coating methods were polymorphous, containing amorphous regions, multiple crystalline phases and incompletely oriented crystallites<sup>1</sup>. While much has been learned about the fundamental nature of ferroelectricity and related properties of polyvinylidene fluoride (PVDF) copolymers, the polymorphous film limits the detail and accuracy of experiments and many questions remained unanswered. The successful fabrication of PVDF copolymers by Langmuir–Blodgett (LB) deposition has resulted in excellent crystalline films as thin as one monolayer<sup>2–5</sup>.

Materials such as metals, polymers, ceramics, ionic crystalline solids, semiconductors, glasses and glass-ceramics interact and respond differently to electromagnetic field; the interaction depends strongly on the microstructure and the type of bonding in the materials<sup>6</sup>.

Whereas polymers and organic materials have been used extensively as dielectric and insulating materials, they have also, in the last decade, taken a prominent place among semiconducting materials, because of their low temperature deposition process and the use of large-area flexible substrates.

Measurement of capacitance of a ferroelectric film reveals many important features connected with the spontaneous polarization, particularly near the phase transition temperature. In the case of ultrathin LB films, the large sample capacitance required analysis of the data to properly account for film conductance, dielectric loss and resistance of the thin film electrode, particularly at high frequencies. The present communication describes the measurements of real ( $\epsilon'$ ) and imaginary ( $\epsilon''$ ) parts of the relative complex permittivity of a 30-monolayer LB film of ferroelectric copolymer of vinylidene fluoride (70%) with trifluoroethylene (30%).

The ultrathin copolymer ferroelectric film was fabricated one monolayer (ML) at a time, by repeatedly dipping a substrate horizontally into a liquid subphase coated with a monolayer of the desired polymer (Schaefer variation of the LB method)<sup>7,8</sup>. The film was deposited at room temperature at a surface pressure of 5 mN/m and consisted of 30 MLs of the copolymer of 70% vinylidene fluoride with 30% trifluoroethylene, p(VDF-TrFF 70:30) deposited on glass with evaporated aluminium electrodes at the top and bottom of the film.

The LB films of 30 ML thickness were mounted in a home-built copper cell assembly with two terminal contacts. The cell temperature was maintained with continuous feedback control and the sample temperature measured with a Cr–Al thermocouple attached to the substrate with silicon heat sink compound. The frequency-dependent capacitance ( $C$ ) and dissipation ( $D \approx \tan \delta$ ) of the sample were measured using Hewlett–Packard 4192 A Impedance Analyser in the frequency range 10 Hz–5 MHz and temperature range 35–125°C. The contact resistance  $R_s$  was measured independently at each temperature by operating the impedance analyser in series mode and extracting the  $R_s$  value in the high frequency limit, as shown in Figure 1. The data were corrected to account for the contact resistance  $R_s$  given in Table 1.

The complex permittivity

$$\epsilon^* = \epsilon' - i\epsilon'' \quad (1)$$

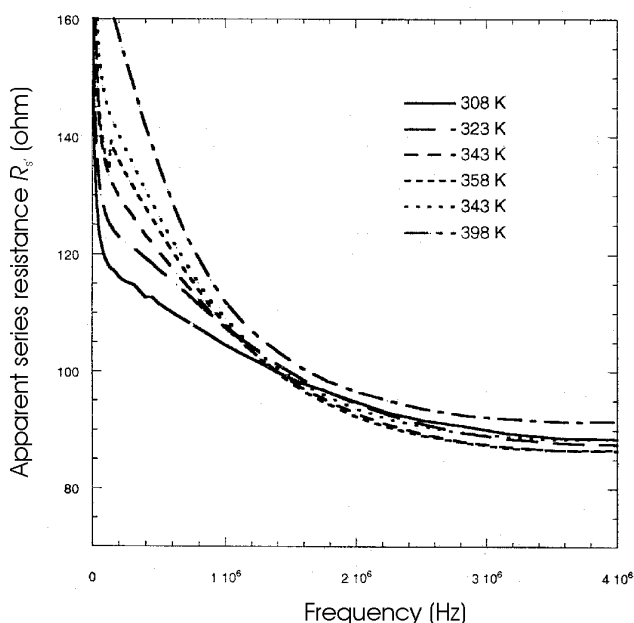


**Figure 1.** Variation of apparent series resistance  $R_s$  with frequency for a 30 ML copolymer sample at different temperatures.

**Table 1.** Contact resistance of samples as a function of temperature in series mode

Temperature (°C)	35	50	70	85	100	125
Series contact resistance $R_s$ (ohm)	88	86	86	84	83	88

<sup>†</sup>For correspondence. (e-mail: mahjogad@rediffmail.com)

was calculated from the parallel-plate capacitor model;

$$\epsilon' = Cd/\epsilon_0 A, \tag{2}$$

$$\epsilon'' = D\epsilon', \tag{3}$$

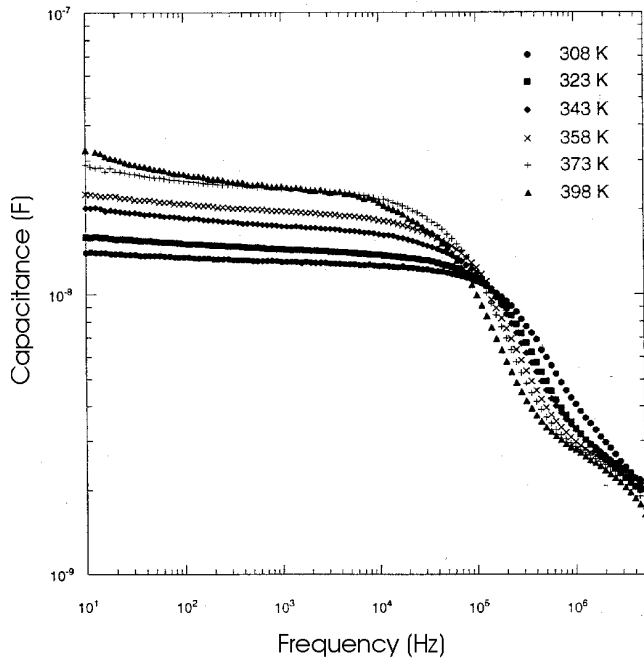


**Figure 2.** Variation of corrected sample capacitance with frequency for the copolymer sample at different temperatures.

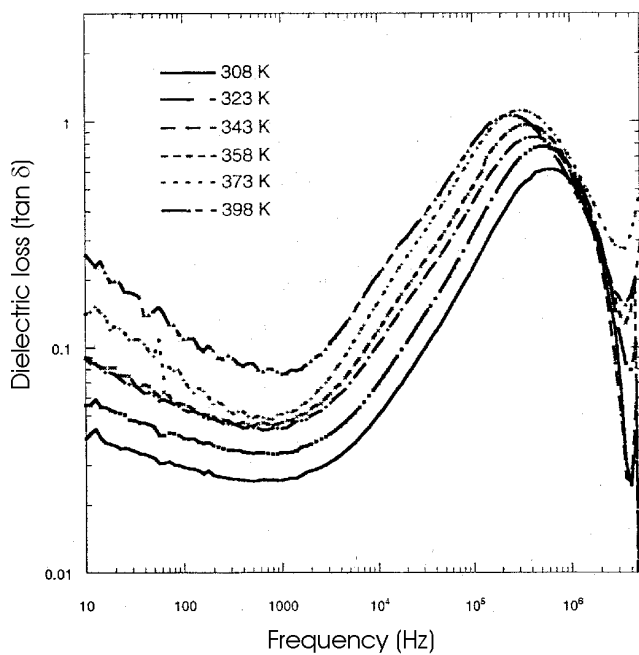


**Figure 3.** Variation of dielectric loss ( $\tan \delta$ ) as a function of frequency for the copolymer sample at different temperatures.

where  $\epsilon_0$  is permittivity of free space,  $A = 18.54 \text{ mm}^2$  is the electrode area,  $d \approx 60 \text{ nm}$  is the sample thickness (assuming 2 nm per ML).

Figure 2 shows the variation of the film capacitance  $C$  with frequency at different temperatures. Figure 3 shows the variation of dissipation factor  $D$  or dielectric loss tangent ( $D = \tan \delta$ ) with frequency at different temperatures. Figure 4a and b shows the variation in  $\epsilon'$  and  $\epsilon''$  with frequency at different temperatures for the ferroelectric polymer sample. The increase  $\epsilon''$  at high frequency, peaking near 250 kHz, is likely due to reso-

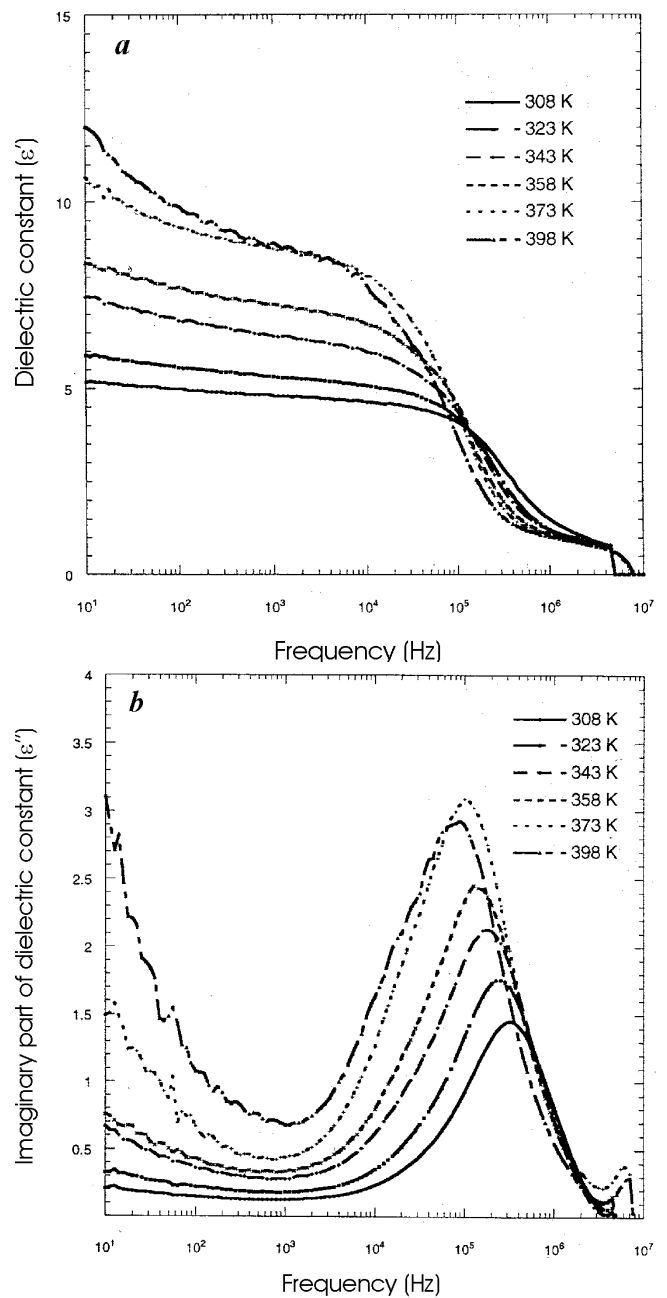


**Figure 4.** Plot of (a) dielectric constant ( $\epsilon'$ ) with frequency and (b) imaginary part of dielectric constant ( $\epsilon''$ ) with frequency for the copolymer sample at different temperatures.

nant loss of the  $\text{CF}_2\text{-CH}_2$  dipoles. This is also evident in the decrease of  $\epsilon'$ , as dipole rotation cannot keep up at high frequency ( $> 10^4$  Hz). This can be attributed to structural rearrangement of the molecule, the  $\alpha$  relaxation process connected with segment motion in polymers<sup>9-16</sup>. The  $\alpha$  process is related to molecular motion in the crystalline region. The other relaxation process is in the amorphous material leading to additional peaks usually located in kHz-MHz region, but these are not evident in

the highly crystalline LB films below the 145°C melting temperature<sup>10</sup>. In the low frequency range ( $< 100$  Hz) the increase in  $\epsilon'$  and  $\epsilon''$  with the decrease in frequency is characteristic of electrical conduction, either by impurity electron and hole conduction, or ionic conduction. In either case, conduction in such a high-resistivity film could lead to injection of space charge coupled with material polarization. The 70:30 copolymer undergoes the ferroelectric to paraelectric structural phase transition

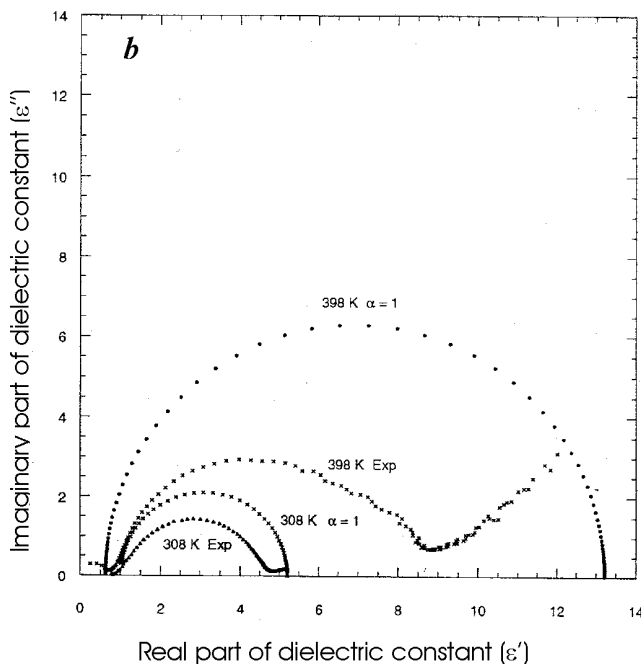
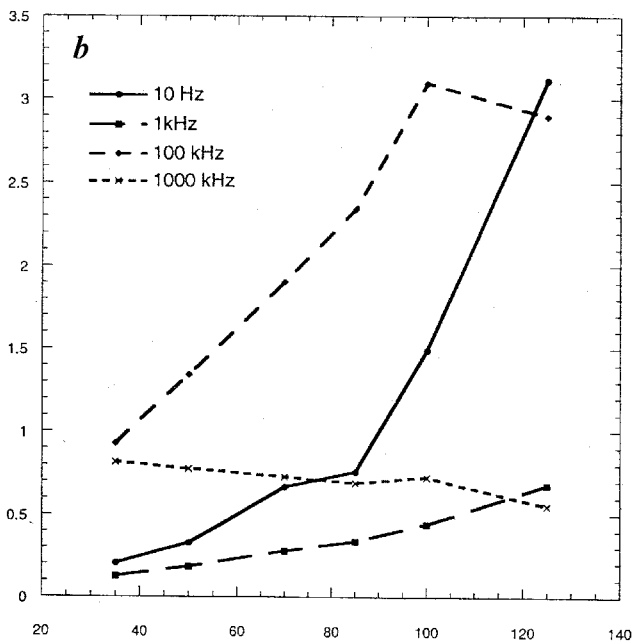
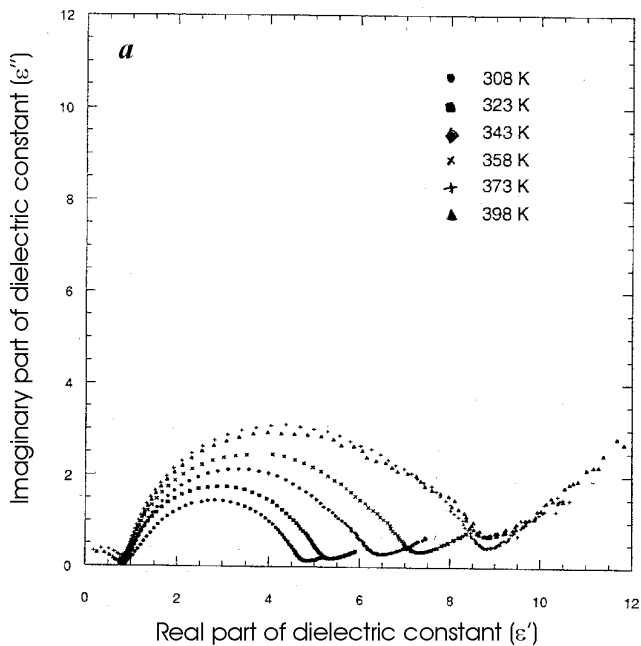
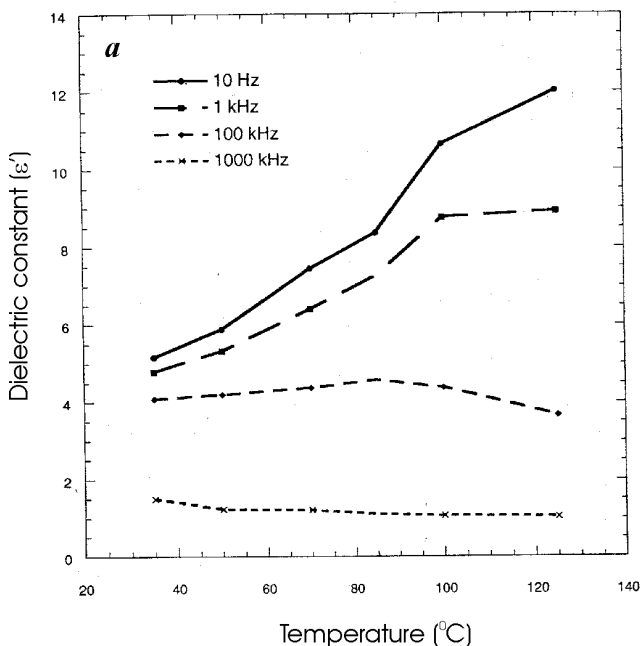


**Figure 5.** Variation of (a) dielectric constant ( $\epsilon'$ ) with temperature and (b) imaginary part of dielectric constant ( $\epsilon''$ ) with temperature at different frequencies for the copolymer sample.

**Figure 6.** Cole-Cole plot of copolymer sample at (a) different temperatures and (b) at 308 and 398 K. Arcs are fitted to Debye formula at  $\alpha=1$ .

at about 100°C on heating<sup>2,3,5</sup>. Since this transition involves the conversion from all-trans molecules conformations to alternating trans-gauche conformations, there should also be increased fluctuations connected with  $\alpha$ -type segmental motion. This trend is evident in the increase of both  $\epsilon'$  (Figure 5a) and  $\epsilon''$  (Figure 5b) at elevated temperature. The effect of the crystalline phase on the complex dielectric constant is further evidence that

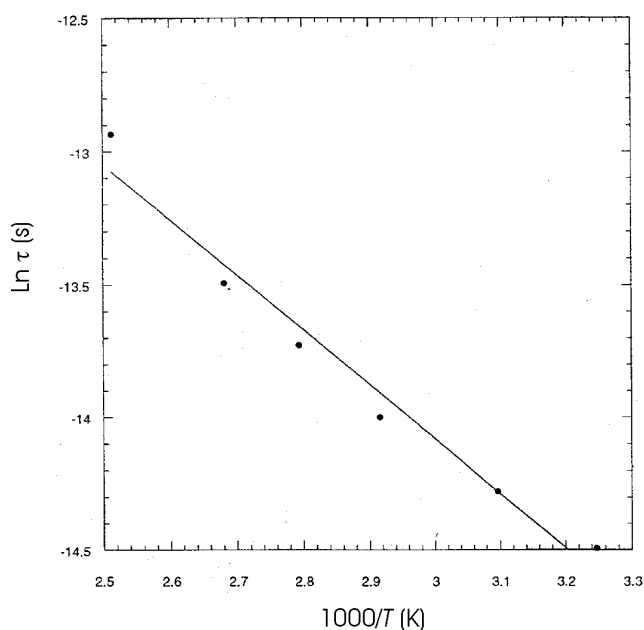


**Figure 7.** Variation of  $\ln \tau$  with reciprocal of absolute temperature for the copolymer sample.

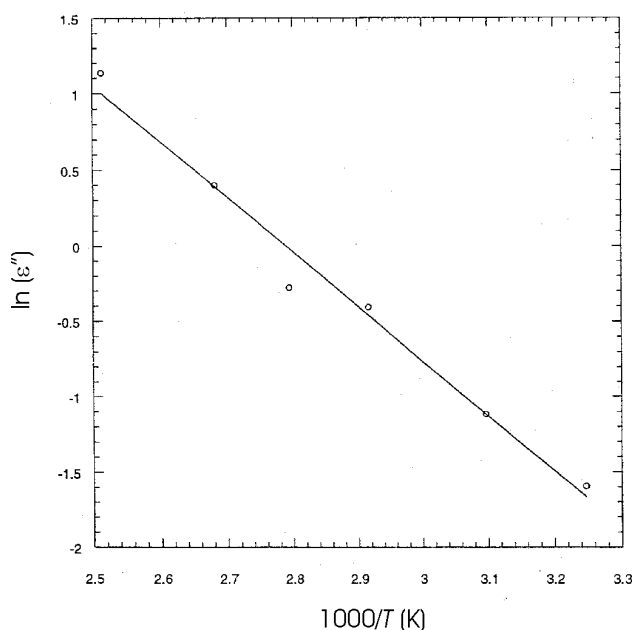


**Figure 8.** Variation of  $\ln(\epsilon'')$  with  $1000/T$  for the copolymer sample at 10 Hz.

the relaxation is likely related mainly to the cooperative orientational movement of the existing dipoles in the polymer chain. The Cole–Cole plot of  $\epsilon''(i\omega)$  vs  $\epsilon'(\omega)$  for the copolymer sample is shown in Figure 6a. The Cole–Cole plot (at  $\alpha=1$ ) at 398 and 308 K is shown in Figure 6b. It is found that the data do not fit well to the relaxation function<sup>17</sup> and the Debye equations as follows:

$$\epsilon''(\omega) = \epsilon(\infty) + \{[\epsilon(s) - \epsilon(\infty)]/[1 + (i\omega t)^{\alpha}]\}, \quad (4)$$

$$\epsilon'(\omega) = \epsilon(\infty) + \{[\epsilon(s) - \epsilon(\infty)]/[1 + (\omega t)^2]\}, \quad (5)$$

$$\epsilon(\omega) = \{[\epsilon(s) - \epsilon(\infty)]/(1 + (\omega t)^2)\}. \quad (6)$$

Equations (5) and (6) can be rewritten as

$$[\epsilon' - (\epsilon_{\infty} + \epsilon_s)/2] + (\epsilon'')^2 = (\epsilon_s - \epsilon_{\infty})^2/4, \quad (7)$$

where  $\omega$  is the angular frequency ( $\omega = 2\pi f$ ),  $\epsilon(\infty)$  is the instantaneous value,  $\epsilon(s)$  is the equilibrium value,  $t$  is the relaxation time, and  $\alpha=1$ , is a parameter expressing a distribution of relaxation times. When there is a distribution of relaxation times, Cole–Cole plot is an arc of a circle with centre below the real axis. At higher temperatures the curves span a longer arc and deviate from the ideal Debye relaxation behaviour. At lower temperatures there is less deviation from Cole–Cole behaviour. It may be recalled that the Cole–Cole plots are semicircles when a single relaxation time is dominant. There is slight shift in relaxation peak towards lower frequency at higher temperature (see Figure 3), indicating an increase relaxation time scale. This is expected for  $\alpha$ -segmental relaxational as fluctuations near the phase transition temperature. The peak of the imaginary part of the dielectric constant  $\epsilon''$  peak (Figure 4b) shifts to lower frequency at elevated temperatures. The relaxation time  $t$  is determined from the frequency  $f_m$  of  $\epsilon''$  peak by the relaxation,  $t = (1/2\pi f_m)$ . Figure 7 shows that the plot of  $\ln t$  (relaxation time) against the reciprocal of absolute temperature. Assuming it is a linear relation, the slope yields the activation energy for dielectric relaxation of 4.1 kcal/mol. Figure 8 shows the variation of  $\ln \epsilon''$  with reciprocal of absolute temperature at a frequency of 10 Hz. It is reasonably linear, with activation energy of 7.21 kcal/mol. This behaviour is often interpreted in terms of the Vogel–Fulcher (VF) model of relaxation near a glass transition<sup>18</sup>. The absence of amorphous material in the LB films<sup>16</sup> means the V–F interpretation may not be quite valid, but the width of the phase transition in the ferroelectric copolymers, implies the dominance of extensive fluctuations which could produce V–F-like behaviour.

The dielectric dispersion exhibits dielectric resonance at about 100 kHz and conductive electronic or ionic loss below 100 Hz. The dielectric resonance is consistent with rotational  $\alpha$ -type motion of the chains and is equivalent

to polarization fluctuations connected with the ferroelectric phase transition at 100°C on heating. The dielectric resonance shows pronounced dispersion, likely due to a distribution of relaxation times.

1. Wang, T. T., Herbert, J. M. and Glass, A. M. (eds), *Applications of Ferroelectric Polymers*, Chapman and Hall, New York, 1988.
2. Palto, S. *et al.*, *Ferro. Lett.*, 1995, **19**, 65.
3. Bune, A. V. *et al.*, *Nature*, 1998, **391**, 874.
4. Blinov, L. M., Fridkin, V. M., Palto, S. P., Bune, A. V., Dowben, P. A. and Ducharme, S., *Phys. Uspekhi*, 2000, **43**, 243.
5. Ducharme, S., Palto, S. P., Blinov, L. M. and Fridkin, V. M., in *Proceedings of the Fundamental Physics of Ferroelectrics* (ed. Cohen, R. E.), American Institute of Physics, Aspen, CO, vol. 535, p. 354.
6. Nguyen, V. Q., Sanghera, J. S., Liyod, I. K., Aggarwal, I. D. and Gershon, D., *J. Non-Cryst. Solids*, 2000, **276**, 151–158.
7. Michael, C. P., *Langmuir – Blodgett Films: An Introduction*, Cambridge University Press, 1996.
8. Ducharme, S., Palto, S. P., Blinov, L. M. and Fridkin, V. M., in *Fundamental Physics of Ferroelectrics* (ed. Cohen, R. E.), AIP Conference Proceedings, AIP Press, Network, 2000, vol. 535, pp. 363.
9. Gregori, R., Jr. and Ueno, E. M., *J. Mater. Sci.*, 1999, **34**, 4489–4500.
10. Johari, G. P. and Goldstein, M., *J. Chem. Phys.*, 1970, **53**, 2372–2388.
11. Yano, S. J., *Polym. Sci.*, 1970, **A2**, 1057.
12. Nakagawa, K. and Ishida, Y., *J. Polym. Sci., Polym. Phys. Ed.*, 1973, **11**, 1503.
13. Furukawa, T., Ohuchi, M., Chiba, A. and Date, M., *Macromolecules*, 1984, **17**, 1394.
14. Hahn, B., Wendorff, J. and Yoon, D. Y., *ibid.*, 1985, **18**, 718.
15. Ando, Y., Hanada, T. and Saitoh, K., *J. Polym. Sci. B: Polym. Phys.*, 1994, **32**, 179.
16. Choi, J. *et al.*, *Phys. Rev.*, 2000, **B61**, 5760.
17. Cole, K. S. and Cole, R. H., *J. Chem. Phys.*, 1941, **9**, 341.
18. Vogel, H., *Phys. Z.*, 1921, **22**, 645–646; Fulcher, G. S., *J. Am. Ceram. Soc.*, 1925, **8**, 339; Tamman, G. and Hesse, W., *Z. Anorg. Allg. Chem.*, 1926, **156**, 245–257.

ACKNOWLEDGEMENTS. M.S.J. thanks the American Physical Society, Kilambi Ramavataram Committee and Fulbright Foreign Scholarship Board for fellowship to work in USA. He also thanks Dr Roger Kirby and Dr Sitaram Jaswal University of Nebraska, Lincoln, USA for encouragement and Dr Meera Chandrasekhar, University of Missouri, Columbia for help while preparing the manuscript. Work at the University of Nebraska was supported by the Nebraska Research Initiative and the National Science Foundation.

Received 3 April 2002; accepted 13 June 2002

## Study of organogenesis *in vitro* from callus tissue of *Flacourtia jangomas* (Lour.) Raeusch through scanning electron microscopy

Indrani Chandra\* and P. Bhanja

Cytogenetics Laboratory, Department of Botany, Burdwan University, Burdwan 713 104, India

***In vitro* regeneration of shoot bud was obtained from nodal segment-derived callus tissue of *Flacourtia jangomas* (Lour.) Raeusch, a woody medicinal plant of dioecious habit. Induction of callus was obtained in MS basal medium supplemented with 2.0 mg/l 2,4-D and 0.5 mg/l BAP. Highest number of shoot bud ( $7.4 \pm 0.20$ ) was noted in 2.0 mg/l BAP. Rhizogenesis was achieved in 1.0 mg/l NAA from both internode and leaf explant. Shoot bud organogenesis was observed through histological and SEM study. Under SEM, several clusters of shoot primordia together with trichomes of characteristic morphology as well as their structural details were noted.**

*FLACOURTIA jangomas* (Lour.) Raeusch (family Flacourtiaceae) is a woody, dioecious plant. It is found frequently in semi-wild conditions in the Brahmaputra valley and adjoining areas in the northeastern parts of India, and had probably migrated from Bangladesh and upper Myanmar. The plant is maintained in forests or orchards elsewhere. This plant has some medicinal as well as economic values. It is mainly cultivated for its edible fruit and hard wood. The fruits are either eaten raw or used for making jams and preserves<sup>1,2</sup>. Different plant parts are also pharmaceutically used for the treatment of asthma, pre- and post-natal blood purification<sup>3</sup>, etc. The fruits are used in bilious conditions and in diarrhoea<sup>4</sup>. The plant contains tannin and a fixed oil<sup>5</sup>. Two limnoids, i.e. limolin and jangomolide have been obtained from its stem and bark<sup>6</sup>. However, no report is available on its *in vitro* organogenesis from callus tissue and its micromorphogenetic responses. Attempts have been made in this paper to investigate the organogenesis from callus tissue and the micromorphogenetic details of the differentiating structures through histological and scanning electron microscope (SEM) studies.

Young internodes (1.0 cm long; 0.1–0.15 cm in diameter; between 3rd and 4th node), nodal segments (0.5 cm long; 0.2 cm in diameter; 4th–5th node) and leaf segments (0.5–0.7 cm<sup>2</sup>; 3rd–4th young unfolded leaves) were taken as explants for callus induction. All these explants were collected from actively growing branches of 10–15-year-old *F. jangomas* trees in Ramana Forest, Golapbag, Burdwan. They were surface sterilized with HgCl<sub>2</sub> (0.1% w/v aqueous) for 5–10 min and washed

\*For correspondence. (e-mail: akalam@cal3.vsnl.net.in)